ISSN 1674-1056
http://cpb.iphy.ac.cn
http://iopscience.iop.org/cpb
中国物理 B
Chinese Physics
中国物理 Chinese Physics B

Improved interfacial properties of HfGdON gate dielectric Ge MOS capacitor by optimizing Gd content

Lin Zhou(周琳)[1], Lu Liu(刘璐)[1], Yu-Heng Deng(邓煜恒)[1], Chun-Xia Li(李春霞)[2], Jing-Ping Xu(徐静平)[1]
Citation: Chin. Phys. B . 2019, 28(12): 127703 . **doi:** 10.1088/1674-1056/ab4e7e
Journal homepage: http://cpb.iphy.ac.cn; http://iopscience.iop.org/cpb

What follows is a list of articles you may be interested in

Improvement of the high-κ/Ge interface thermal stability using an *in-situ* ozone treatment characterized by conductive atomic force microscopy

Ji-Bin Fan(樊继斌), Xiao-Jiao Cheng(程晓姣), Hong-Xia Liu(刘红侠), Shu-Long Wang(王树龙), Li Duan(段理)
Chin. Phys. B . 2017, 26(8): 087701 . **doi:** 10.1088/1674-1056/26/8/087701

Influences of different oxidants on characteristics of La_2O_3/Al_2O_3 nanolaminates deposited by atomic layer deposition

Ji-Bin Fan(樊继斌), Hong-Xia Liu(刘红侠), Li Duan(段理), Yan Zhang(张研), Xiao-Chen Yu(于晓晨)
Chin. Phys. B . 2017, 26(6): 067701 . **doi:** 10.1088/1674-1056/26/6/067701

Performance and reliability improvement of La_2O_3/Al_2O_3 nanolaminates using ultraviolet ozone post treatment

Ji-Bin Fan(樊继斌), Hong-Xia Liu(刘红侠), Bin Sun(孙斌), Li Duan(段理), Xiao-Chen Yu(于晓晨)
Chin. Phys. B . 2017, 26(5): 057702 . **doi:** 10.1088/1674-1056/26/5/057702

Crystallization behaviors of ultrathin Al-doped HfO_2 amorphous films grown by atomic layer deposition

Xue-Li Ma(马雪丽), Hong Yang(杨红), Jin-Juan Xiang(项金娟), Xiao-Lei Wang(王晓磊), Wen-Wu Wang(王文武), Jian-Qi Zhang(张建齐), Hua-Xiang Yin(殷华湘), Hui-Long Zhu(朱慧珑), Chao Zhao(赵超)
Chin. Phys. B . 2017, 26(2): 027701 . **doi:** 10.1088/1674-1056/26/2/027701

Electron trapping properties at HfO_2/SiO_2 interface, studied by Kelvin probe force microscopy and theoretical analysis

Man-Hong Zhang(张满红)
Chin. Phys. B . 2016, 25(8): 087701 . **doi:** 10.1088/1674-1056/25/8/087701

Improved interfacial properties of HfGdON gate dielectric Ge MOS capacitor by optimizing Gd content*

Lin Zhou(周琳)[1], Lu Liu(刘璐)[1], Yu-Heng Deng(邓煜恒)[1], Chun-Xia Li(李春霞)[2], and Jing-Ping Xu(徐静平)[1,†]

[1] School of Optical and Electronic Information, Huazhong University of Science and Technology, Wuhan 430074, China
[2] Shenzhen Institute of Information Technology, Shenzhen 518172, China

(Received 5 July 2019; revised manuscript received 24 September 2019; published online 22 November 2019)

High-quality dielectric/Ge interface and low gate leakage current are crucial issues for high-performance nanoscaled Ge-based complementary metal–oxide–semiconductor (CMOS) device. In this paper, the interfacial and electrical properties of high-k HfGdON/LaTaON stacked gate dielectric Ge metal–oxide–semiconductor (MOS) capacitors with different gadolinium (Gd) contents are investigated. Experimental results show that when the controlling Gd content is a suitable value (*e.g.*, $\sim$ 13.16%), excellent device performances can be achieved: low interface-state density (6.93×10^{11} cm^{-2}·eV^{-1}), small flatband voltage (0.25 V), good capacitance–voltage behavior, small frequency dispersion, and low gate leakage current (2.29×10^{-6} A/cm^2 at $V_g = V_{fb} + 1$ V). These could be attributed to the repair of oxygen vacancies, the increase of conduction band offset, and the suppression of germanate and suboxide GeO_x at/near the high k/Ge interface by doping suitable Gd into HfON.

Keywords: Ge MOS devices, HfGdON dielectric, interface quality, leakage current density

PACS: 77.55.D–, 77.55.dj, 77.55.F–, 81.15.–z **DOI:** 10.1088/1674-1056/ab4e7e

1. Introduction

Recently, it has become increasingly difficult in further scaling down the geometric dimension of Si-based metal–oxide–semiconductor field-effect transistor (MOSFET). For overcoming the obstacle, Ge-based and III–V compound semiconductor-based MOSFETs (*e.g.*, GaN-HEMTs) with high-k gate dielectric have been extensively studied to further improve the scaled CMOS technology due to their higher electron and/or hole mobilities than those of silicon.[1–6] For Ge MOS, unstable and water-soluble GeO_x ($x < 2$) degrades the Ge/gate-dielectric interface quality, resulting in poor electrical properties,[7] which has hampered the development of Ge MOSFET. In order to solve this problem, different surface passivation layers, such as LaTaON,[8] ZrON,[9] NbSiON,[10] *etc*.[11–14] have been investigated and exhibited good interface quality in the presence of Ge. On the other hand, Hf-based oxide has been considered as one of the most promising high-k materials and used as gate dielectric due to its high k value ($\sim$ 25) and large band gap ($\sim$ 5.8 eV).[15,16] However, it has been found that the electrical properties of the device will be degraded due to intermixing between Ge and Hf.[1,2,7–14] Although the incorporation of nitrogen (N) into HfO_2 could suppress Ge and O diffusion and improve the interfacial property,[17,18] it reduced the valence- and conduction-band offsets.[19] Fortunately, some recent investigations have demonstrated that the Gd-doped HfO_2 can increase the conduction-band offset and transform HfO_2 from the monoclinic phase to the cubic phase, thus diminishing the leakage, improving the interface quality, and also augmenting the k value of dielectric.[20,21] So in this work, the effects of Gd content in HfGdON gate dielectric on interface and electrical properties of Ge MOS devices with LaTaON interlayer are further investigated so that Gd content is optimized to obtain high-quality dielectric/Ge interface and excellent device performances.

2. Experiments

Ge MOS capacitors were fabricated on (100) n-type Ge wafers with a resistivity of 0.02 Ω·cm–0.1 Ω·cm. The wafers were cleaned by using ethanol, acetone, and trichloroethylenein in sequence, followed by dipping them in diluted HF (1 : 50) for 30 s, and then rinsed with deionized water for several cycles to remove the native oxide. After drying by N_2, the wafers were transferred immediately to the vacuum chamber of a sputtering system. Before deposition, the vacuum chamber was evacuated to a base pressure of 5.0×10^{-4} Pa. A $\sim$ 2-nm LaTaN film was deposited by cosputtering of La target and Ta target at room temperature in an Ar/N_2 (= 15/6) ambient atmosphere, followed by an *in-situ* deposition of $\sim$ 8-nm HfGdON film by cosputtering of HfO_2 target and Gd target in the same ambient. The Gd content was adjusted by changing the Gd-target power as shown in Fig. 1. Then, a postdeposition annealing (PDA) was carried out in N_2 (500 sccm)+O_2 (50 sccm) ambient atmosphere at 500 °C for 5 min to convert

*Project supported by the National Key Research and Development Program of China (Grant No. 2018YFB2200500) and the National Natural Science Foundation of China (Grant Nos. 61851406 and 61274112).

†Corresponding author. E-mail: jpxu@hust.edu.cn

© 2019 Chinese Physical Society and IOP Publishing Ltd

LaTaN into LaTaON and reduce the oxygen vacancy in HfGdON film. The Al was thermally evaporated and patterned by lithography, and used as a gate electrode with an area of 7.85×10^{-5} cm^2. Finally, postmetallization annealing was carried out in a forming gas (95% N_2+5% H_2) at 300 °C for 20 min.

High-frequency (HF, 1 MHz) capacitance–voltage (*C*–*V*) and gate leakage current density *versus* gate voltage (J_g–V_g) characteristics were measured by HP4284A precision LCR meter and Keithley 4200-SCS semiconductor parameter analyzer respectively under a light-tight and electrically-shielded condition at room temperature. The physical thickness of the gate dielectric was determined by a spectroscopic ellipsometer. The x-ray photoelectron spectroscopy (XPS) was employed to investigate the compositions and chemical states of the samples.

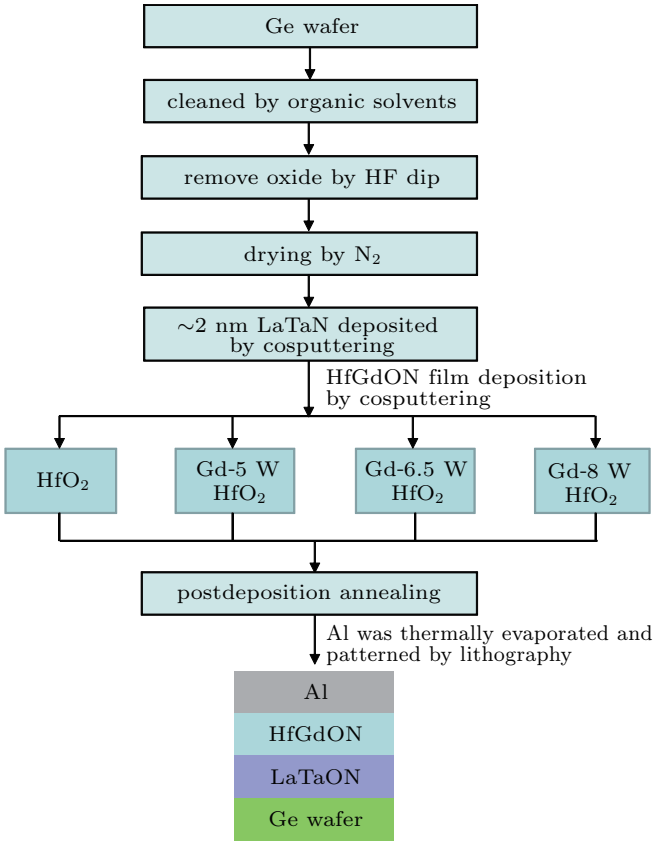


Fig. 1. Process flow chart of Ge MOS capacitor with gate stacked dielectric of HfGdON/LaTaON/Ge.

3. Results and discussion

The compositions and chemical states of four samples with different Gd contents (from 0 to 45%, as analyzed below) are investigated by etching the HfGdON gate dielectrics to a thickness of ~ 4 nm from the Ge surface using an *in-situ* Ar^+ ion beam in the XPS chamber. The binding energy is calibrated by centering the Ge 3d at 28.8 eV, and all peaks have their own fixed full wide at half maximum (FWHM). Firstly, the spectrum of La 3d is shown in Fig. 2(a), and two strong peaks at 851.40 eV (La $3d_{3/2}$) and 834.50 eV (La $3d_{5/2}$) are detected. The spin–orbit splitting energy of 16.9 eV is in a good accordance with that of La_2O_3/LaON, and the La $3d_{3/2}$ peaks related to La_2O_3 are located in a binding-energy range of 834.2 eV–837.0 eV,[21] confirming the presence of La_2O_3/LaON in the interlayer. The spectrum of Ta 4f is shown in Fig. 2(b), in which two strong peaks are located at 26.18 eV (Ta $4f_{7/2}$) and 28.01 eV (Ta $4f_{5/2}$), respectively. The spin–orbit splitting energy is 1.83 eV, which is close to a standard value of 1.9 eV, indicating the presence of Ta^{5+} from Ta_2O_5/TaON.[22]

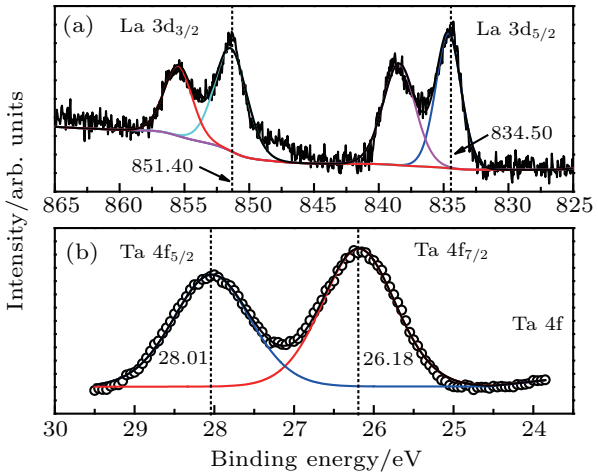


Fig. 2. XPS spectrum of HfGdON/LaTaON/Ge MOS with Gd content of ~ 13.16% for (a) La 3d and (b) Ta 4f. Other samples with Gd incorporation have similar results.

The Gd 4d core-level spectrum is shown in Fig. 3(a), and two strong peaks of Gd $4d_{3/2}$ (~ 147.47 eV) and Gd $4d_{5/2}$ (~ 142.43 eV) are detected, which can be fitted well by spin–orbit splitting energy of about 5.0 eV, confirming the formation of Gd_2O_3/GdON.[23] In addition, an extra peak (~ 140.65 eV) can be observed, which can be attributed to the electrostatic interaction between Gd 4d core level and a partially filled Gd 4f level because Gd belongs to the heavy lanthanide group element.[24] Figure 3(b) is the N 1s spectrum, showing the incorporation of nitrogen into the gate dielectric film.

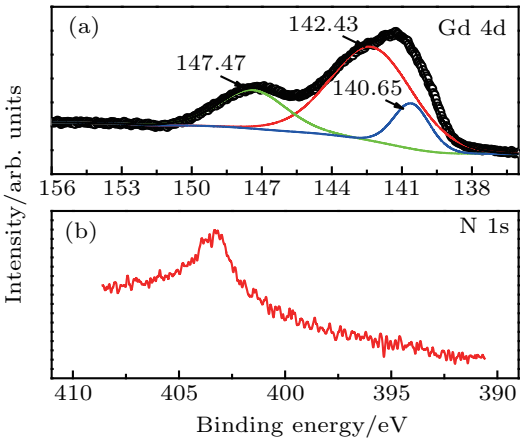


Fig. 3. XPS spectra of HfGdON/LaTaON/Ge MOS with Gd content of ~ 13.16% for (a) Gd 4d and (b) N 1s. Other Gd-doped samples have similar results.

Figure 4 demonstrates the core-level spectra of Hf 4f, and all of them are deconvoluted into two peaks of Hf $4f_{5/2}$ and Hf $4f_{7/2}$, which are in accordance with spin–orbit splitting energy of about 1.7 eV.[25–27] From the above XPS results, it can be suggested that the HfGdON dielectric film is formed. By calculating the peak-area ratio of Gd 4d to Hf 4f for each of the three Gd-doped samples, their Gd content values [Gd/(Gd+Hf)] are obtained to be 13.16%, 29.86%, and 45.47%, respectively. Compared with the control sample without doping Gd, the sample with the Gd content of $\sim$ 13.16% possesses a 0.2-eV binding energy shift of the Hf 4f peak, which, obviously, is caused by the incorporation of gadolinium into HfON film. As the Gd/(Gd+Hf) atomic ratio increases, the Hf 4f peaks shift to higher binding energy, which is consistent with the results in Refs. [28] and [29] and can be attributed to the suppression of oxygen vacancies by doping Gd, to reduce the local electronic density of states.[20,28,30]

Because of a strong overlap between the Ge 3d peak and Hf or Ta peak,[8,31] the Ge $2p_{3/2}$ core level spectrum for each of four samples is used to investigate interfacial quality between the high-k stack and Ge substrate as shown in Fig. 5. The peaks from GeO_2, GeO_x, and Ge substrates are found to be located at 1221.1 eV, 1218.8 eV, and 1217.5 eV,[32] respectively. For the Gd-doped samples, a peak with a binding energy (BE) value of 1216.2 eV is observed, which belongs to Gd $3d_{3/2}$ whose BE value is between 1212 eV and 1227 eV.[33] A peak with a BE value of 1219.9 eV in Fig. 4(a) originates from $HfGeO_x$, which is formed due to the Hf and O diffusing onto the surface of Ge substrate during the 500-°C PDA.[34] The O 1s core level spectra of four samples in Fig. 6 further confirm the formation of $HfGeO_x$ and Ge suboxides as indicated by the Ge–O–Hf and O–Ge peaks, respectively. The $HfGeO_x$ peak has a positive shift of BE ($\Delta_{BE} = 2.40$ eV) relative to the peak of the Ge substrate as shown in Fig. 5(a). Obviously, as Gd content increases from 0 to 13.16%, this shift decreases ($\Delta_{BE} = 1.76$ eV), indicating the suppression of the Hf diffusion by Gd incorporation. However, as Gd content increases to higher values, a turnaround of Δ_{BE} occurs, indicating the augment of the germanate due to the distortion of crystal structure by excessive Gd incorporation (29.86% and 45.47%).[35] To further analyze the effects of Gd doping, the area ratios of Ge suboxide to Ge 2p peak for four samples are calculated to be 12.06%, 5.39%, 7.72%, and 10.85%,

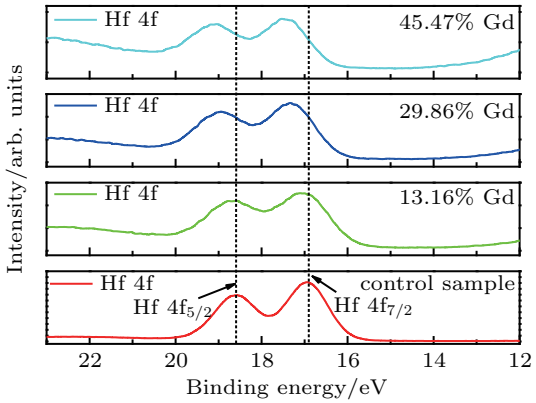


Fig. 4. XPS spectra of Hf 4f for four samples with (a) 0% Gd, (b) 13.16% Gd, (c) 29.86% Gd, and (d) 45.47% Gd.

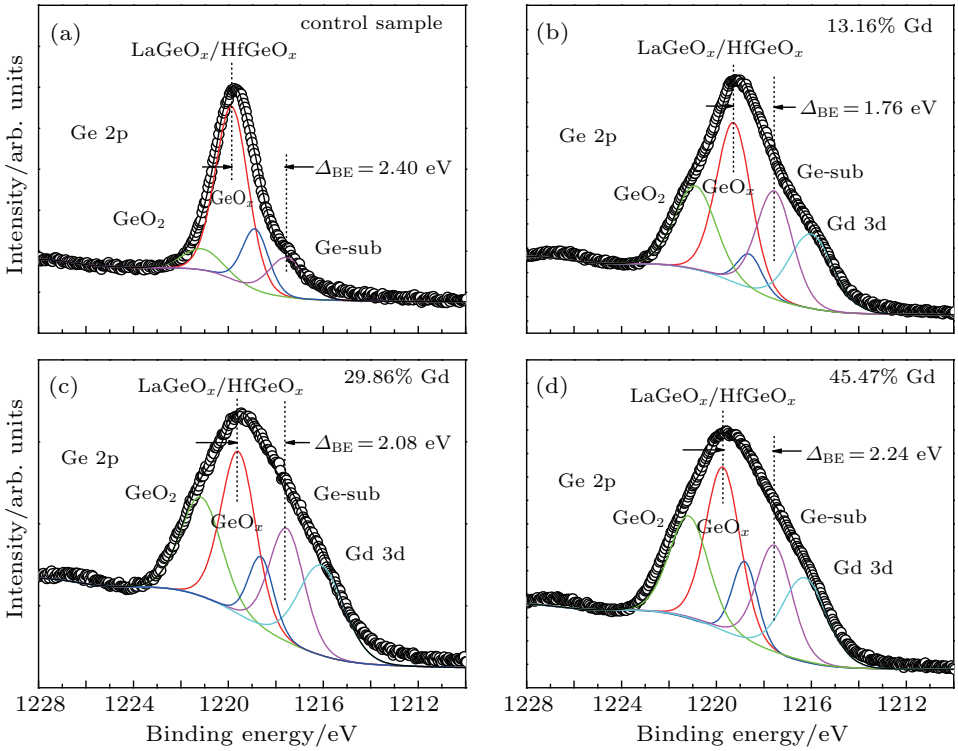


Fig. 5. XPS spectra of Ge 2p for four samples with (a) 0% Gd, (b) 13.16% Gd, (c) 29.86% Gd, and (d) 45.47% Gd.

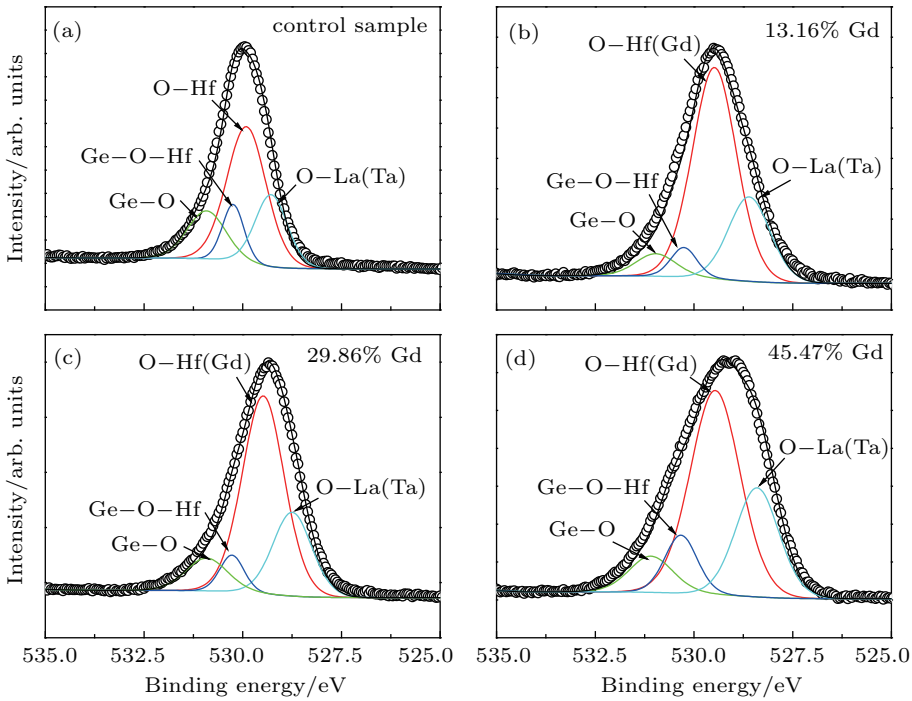


Fig. 6. XPS spectra of O 1s for four samples with (a) 0% Gd, (b) 13.16% Gd, (c) 29.86% Gd, and (d) 45.47% Gd.

corresponding to the samples with Gd content increasing from 0% to 45.47% respectively, implying that the formation of the unstable GeO_x can greatly be suppressed due to an effective blocking role of Gd against O diffusion for the sample with Gd content of 13.16%, and however, with the incorporation of excessive Gd, *e.g.*, 29.86%, even 45.47%, the peak area ratio of GeO_x gradually increases and the interface quality is degraded due to the increased O diffusion. The peak intensity of the O–Ge bond in O 1s XPS spectra presents the same change trend in Fig. 6.

Based on the above XPS analyses, it can be suggested that the incorporation of an appropriate amount of Gd into HfON can suppress the formation of germanate and suboxide GeO_x, and however, excessive Gd incorporation into HfON will be counterproductive. So it is important to control the Gd content entering into HfON for the purpose of improving the interfacial quality between HfGdON dielectric and Ge substrate.

Figure 7 demonstrates the typical HF *C*–*V* curves of the control sample (HfON) and three HfGdON samples. Apparently, the control sample has a much smaller accumulation capacitance (C_{ox}) than those HfGdON samples, indicating that the incorporation of Gd into the HfON dielectric can increase its permittivity (k). The increased k value is attributed to the transformation of crystal structure wherein Gd^{3+} replaces a part of Hf^{4+}. As is well known, the ionic radius of Gd^{3+} (~ 0.105 nm) is slightly larger than that of Hf^{4+} (~ 0.08 nm), which increases the length of the anion–cation bond, resulting in the enhancement of the molecular polarizability.[36]

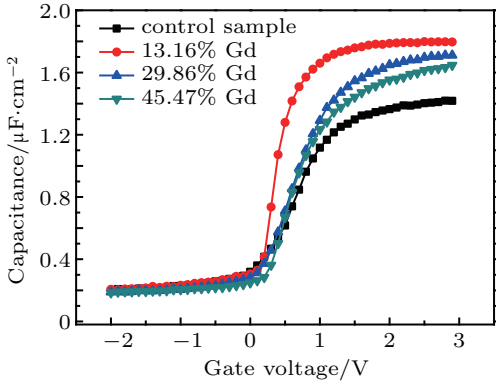


Fig. 7. Typical HF *C*–*V* curves of four samples with different amounts of Gd.

The permittivity can be calculated from[37] $k = (1 + 8\pi a_m/3V_m)/(1 - 4\pi a_m/3V_m)$ where a_m denotes the molecular polarizability and V_m is the molecular volume. Obviously, the k value of HfGdON dielectric increases with the molecular polarizability increasing. In addition, the k value of the monoclinic HfO_2 is lower than that of the cubic HfO_2. With the Gd incorporation, the content of longer O–Gd bond increases as confirmed by the XPS spectrum of O 1s, and the monoclinic HfO_2 is transformed into the cubic HfO_2 due to substitution of O–Gd for O–Hf,[20] which plays a role in increasing k value too. But the k value will not always increase with the Gd content increasing as demonstrated by the measured results. The extracted electrical parameters from the *C*–*V* curves are listed in Table 1. The equivalent k value of the gate dielectric is calculated from $k = C_{ox}t_{ox}/\varepsilon A$, where t_{ox} is the thickness of gate dielectric and A is the area of capacitor.

The value of V_{fb} is determined by the flat-band capacitance,[38] and the oxide-charge density (Q_{ox}) is calculated from $Q_{ox} = -C_{ox}(V_{fb} - \phi_{ms})/q$, where ϕ_{ms} is the work-function difference between Al and Ge. The interface-state density near midgap (D_{it}) is estimated by the Terman's method.[39] Obviously, the k value increases firstly and decreases then as the Gd content increases, and reaches a maximum value (~ 20.5) for Gd content of $\sim 13.16\%$. the k value for the samples decreasing with excessive Gd doping can be attributed to lower permittivity of the pure Gd_2O_3 than that of HfO_2.

Table 1. Electrical and physical parameters extracted from the HF C–V curve of four samples.

$Hf_{1-x}Gd_xON$	k	$D_{it}/cm^{-2}\cdot eV^{-1}$	V_{fb}/V	$J_g/(A/cm^2)@V_g = V_{fb}+1$ V	Q_{ox}/cm^{-2}
Gd (0%)	16.04	6.98×10^{12}	0.44	5.73×10^{-4}	-3.74×10^{12}
Gd (13.16%)	20.51	6.93×10^{11}	0.25	2.29×10^{-6}	-2.73×10^{12}
Gd (29.86%)	18.87	2.82×10^{12}	0.36	1.39×10^{-5}	-2.99×10^{12}
Gd (45.47%)	18.61	5.59×10^{12}	0.41	1.38×10^{-4}	-3.36×10^{12}

The hysteresis behaviors of the C–V curves for the four samples are presented in Fig. 8. To quantify their differences, the hysteresis voltages are calculated each as an averaged value between 0 V and 1 V, which, specifically,are 168 mV, 13 mV, 17 mV, and 20 mV for the samples with increasing Gd content. Compared with the control sample, the Gd-doped samples exhibit small hysteresis, implying a low density of defects in the LaTaON IPL and near/at the HfGdON/LaTaON interface due to the suppression of oxygen vacancies by doping Gd.[35] But for excessive Gd content, the crystal structure is distorted, resulting in the formation of more germinate and GeO_x near/at the high-k/Ge interface due to enhanced diffusion of Hf and O towards the Ge surface as confirmed by the above XPS analyses, thus increasing hysteresis.

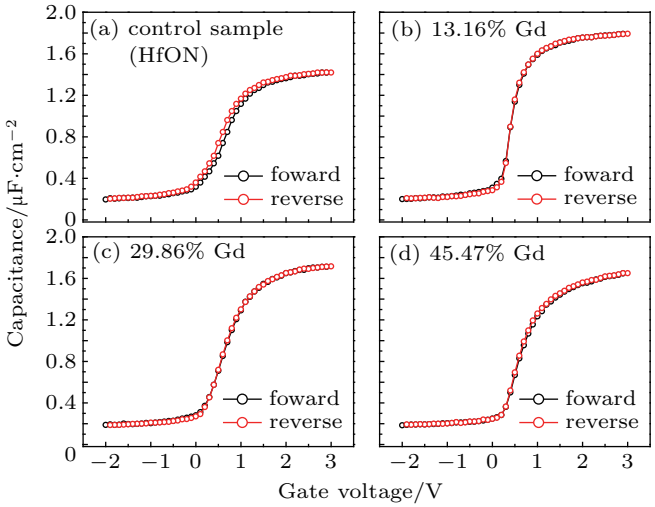


Fig. 8. Hystereses of C–V curves for four samples with (a) 0% Gd, (b) 13.16% Gd, (c) 29.86% Gd, and (d) 45.47% Gd.

To further illustrate the interface quality of the samples, the frequency dispersions of the C–V curves for the four samples are shown in Fig. 9. Once again, the sample with Gd content of $\sim 13.16\%$ exhibits the smallest frequency dispersion, and as Gd content increases, the frequency dispersion gradually becomes bigger due to the same causes as the above, indicating the excellent interface quality for the 13.16%-Gd sample, which is further supported by its smallest D_{it} as listed in Table 1.

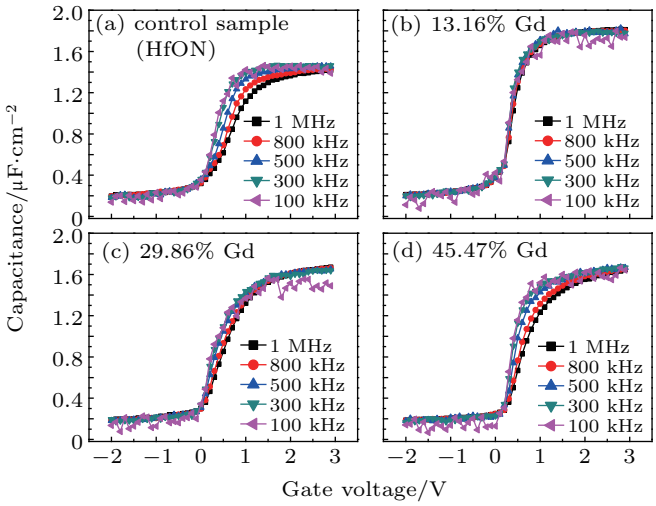


Fig. 9. Frequency dispersion of C–V curves for four samples with (a) 0% Gd, (b) 13.16% Gd, (c) 29.86% Gd, and (d) 45.47% Gd.

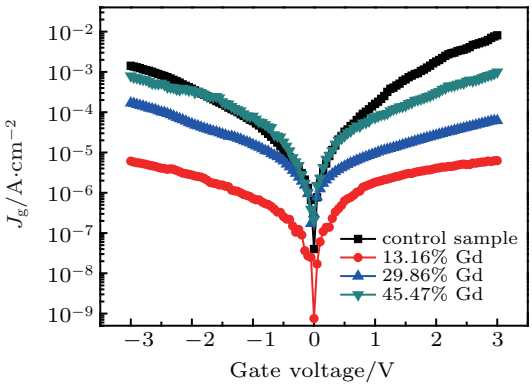


Fig. 10. Plots of gate leakage current density *versus* gate voltage for four samples.

Figure 10 shows typical gate leakage properties of the four samples. The leakage current densities of all the Gd-doped samples are lower than that of the control sample due to the increase of conduction-band offset (ΔE_c)[20] and the decrease of oxygen vacancies in the HfGdON film to different amounts. Furthermore, the lower electronegativity (~ 1.2)

and larger ionic radius (~ 0.105 nm) of Gd^{3+} also contribute to the decrease of leakage current for the Gd-doped samples. However, the quantity of Gd^{3+} substitution for Hf^{4+} increases with Gd content increasing, which causes lattice to distort. Consequently, the 13.16%-Gd sample has the lower gate-leakage current than other Gd-doped samples (*e.g.*, at $V_g = V_{fb} + 1$ V, $J_g = 5.73 \times 10^{-4}$ A/cm^2, 2.29×10^{-6} A/cm^2, 1.39×10^{-5} A/cm^2, and 1.38×10^{-4} A/cm^2 for the samples with increasing Gd contents respectively, as listed in Table 1), which is ascribed to its better interface quality and suppressed formation of Ge suboxide as confirmed by the above XPS analyses.

In addition, the AFM images of the gate–dielectric surface of all the samples are shown in Fig. 11. The root-mean-square (RMS) values of their surface roughness are 0.544, 0.206, 0.23, and 0.437 for the control sample and the samples with Gd contents of 13.16%, 29.86%, and 45.47%, respectively. With Gd incorporation, the HfGdON surface becomes smoother, but the excessive Gd incorporation generates the larger lattice strain in HfGdON due to substitutional increase, leading to larger RMS value. In fact, there is a one-to-one correspondence between the surface roughness and the gate leakage current or interface-state density, as shown by the above experimental results.

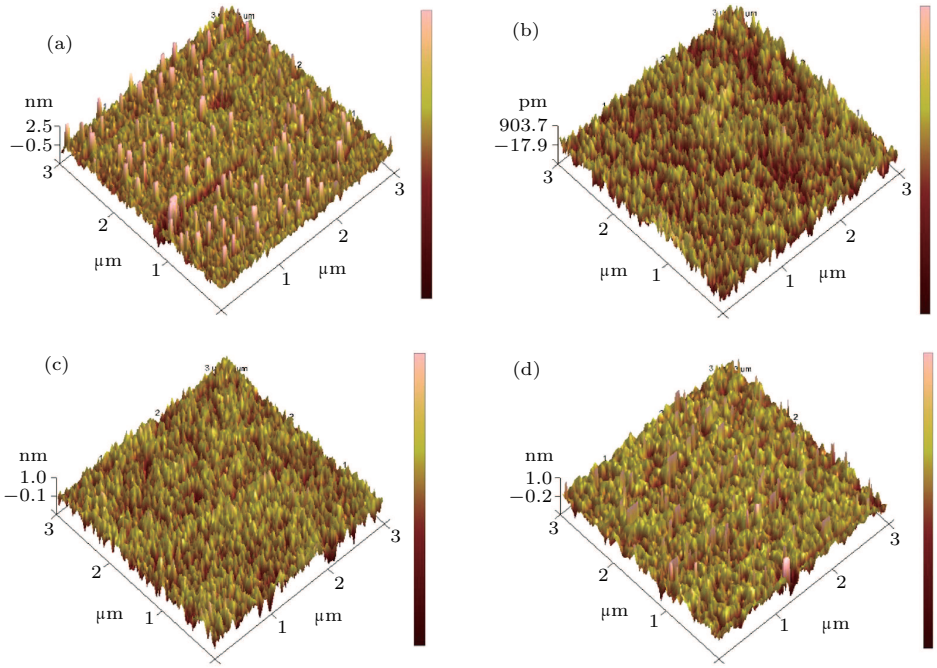


Fig. 11. AFM images of gate–dielectric surface for four samples with (a) 0% Gd, (b) 13.16% Gd, (c) 29.86% Gd, and (d) 45.47% Gd.

4. Conclusions

In summary, the effects of the Gd content in HfGdON gate dielectric on interfacial and electrical properties of the Ge MOS capacitor with LaTaON as interlayer are investigated. It is found that reasonable Gd incorporation in HfON (*e.g.*, $\sim$ 13.16% Gd) exhibits superior interfacial and electrical properties, which is due to the formation of less germanate and the suppression of unstable Ge suboxides. Furthermore, the Gd-doped HfON can obtain larger conduction band offset (ΔE_c) and effectively suppress the formation of oxygen vacancies, which contributes to small gate leakage current (2.29×10^{-6} A/cm^2 at $V_g = V_{fb} + 1$ V) and low interface-state density (6.93×10^{11} cm^{-2}·eV^{-1}) for the 13.16%-Gd sample. However, when excessive Gd is incorporated, the performance of the device is deteriorated due to the distortion of crystal structure and poor interface quality. For Gd content below 13.16%, it deserves to further investigate their effects on device performances for determining the optimal Gd content in the gate stacked dielectric of HfGdON/LaTaON, and thus achieving more excellent electrical performance of Ge MOS device.

References

[1] Chi On C, Kim H, Chi D, McIntyre P C and Saraswat K C 2006 *IEEE T. Electron Dev.* **53** 1509
[2] Kamata Y 2008 *Mater. Today* **11** 30
[3] Chen D, Liu Z, Lu X, Wan L, Li R, Yang Z and Li G 2019 *J. Mater. Chem. C* **7** 2823
[4] Chen D, Wan L, Li J, Liu Z and Li G 2019 *Solid State Electron.* **151** 60
[5] Kong X T, Zhou X L, Li S Y, Qiao L J, Liu H G, Wang W and Pan J Q 2015 *Chin. Phys. Lett.* **32** 037301
[6] Zhang T, Pu T, Xie T, Li L, Bu Y, Wang X and Ao J P 2018 *Chin. Phys. B* **27** 078503
[7] Caymax M, Houssa M, Pourtois G, Bellenger F, Martens K, Delabie A and Van Elshocht S 2008 *Appl. Surf. Sci.* **254** 6094
[8] Feng J, Jing-Ping X, Yong H, Lu L and Lai P T 2014 *IEEE T. Electron Dev.* **61** 3608
[9] Yuan W, Xu J, Liu L, Huang Y and Cheng Z 2016 *Semiconductors +* **37** 054004
[10] Huang Y, Xu J P, Liu L, Lai P T and Tang W M 2016 *Appl. Phys. Lett.* **109** 193504
[11] Chui C O, Ito F and Saraswat K C 2004 *IEEE T. Electron Dev.* **25** 613

[12] Gao F, Lee S J, Pan J S, Tang L J and Kwong D L 2005 *Appl. Phys. Lett.* **86** 113501
[13] Kim K H, Gordon R G, Ritenour A and Antoniadis D A 2007 *Appl. Phys. Lett.* **90** 212104
[14] Li C X and Lai P T 2009 *Appl. Phys. Lett.* **95** 022910
[15] Cockayne E 2008 *J. Appl. Phys.* **103** 084103
[16] Zhu H, Tang C, Fonseca L R C and Ramprasad R 2012 *J. Mater. Sci.* **47** 7399
[17] Xu H X, Xu J P, Li C X and Lai P T 2010 *Appl. Phys. Lett.* **97** 022903
[18] Lin M H, Lan C K, Chen C C and Wu J Y 2011 *Appl. Phys. Lett.* **99** 182105
[19] Sayan S, Nguyen N V, Ehrstein J, Chambers J J, Visokay M R, Quevedo-Lopez M A, Colombo L, Yoder D, Levin I, Fischer D A, Paunescu M, Celik O and Garfunkel E 2005 *Appl. Phys. Lett.* **87** 212905
[20] Wang L G, Xiong Y, Xiao W, Cheng L, Du J, Tu H and van de Walle A 2014 *Appl. Phys. Lett.* **104** 201903
[21] Huang X D, Sin J K O and Lai P T 2012 *IEEE T. Device Mater. Rel.* **12** 306
[22] Chun W J, Ishikawa A, Fujisawa H, Takata T, Kondo J N, Hara M, Kawai M, Matsumoto Y and Domen K 2003 *J. Phys. Chem. B* **107** 1798
[23] Uwamino Y, Ishizuka T and Yamatera H 1984 *J. Electron. Spectrosc.* **34** 67
[24] Datta P, Majewski P and Aldinger F 2009 *Mater. Charact.* **60** 138
[25] Dai J Y, Lee P F, Wong K H, Chan H L W and Choy C L 2003 *J. Appl. Phys.* **94** 912
[26] Yamamoto K, Hayashi S, Niwa M, Asai M, Horii S and Miya H 2003 *Appl. Phys. Lett.* **83** 2229
[27] Sahiner M A, Woicik J C, Gao P, McKeown P, Croft M C, Gartman M and Benapfla B 2007 *Thin Solid Films* **515** 6548
[28] Xiong Y, Tu H, Du J, Ji M, Zhang X and Wang L 2010 *Appl. Phys. Lett.* **97** 012901
[29] Losovyj Y B, Ketsman I, Sokolov A, Belashchenko K D, Dowben P A, Tang J and Wang Z 2007 *Appl. Phys. Lett.* **91** 132908
[30] Ketsman I, Losovyj Y B, Sokolov A, Tang J, Wang Z, Belashchenko K D and Dowben P A 2007 *Appl. Phys. A* **89** 489
[31] Lee J J, Shin Y, Choi J, Kim H, Hyun S, Choi S, Cho B J and Lee S H 2012 *Phys. Status Solid-R* **6** 439
[32] Prabhakaran K and Ogino T 1995 *Surf. Sci.* **325** 263
[33] Glorieux B, Berjoan R, Matecki M, Kammouni A and Perarnau D 2007 *Appl. Surf. Sci.* **253** 3349
[34] Li X F, Liu X J, Cao Y Q, Li A D, Li H and Wu D 2013 *Appl. Surf. Sci.* **264** 783
[35] Jiang S S, He G, Fang Z B, Wang P H, Liu Y M, Lv J G and Liu M 2018 *J. Alloys Compd.* **757** 288
[36] Joshi P C, Krupanidhi S B and Mansingh A 1992 *J. Appl. Phys.* **72** 5517
[37] Rahman M S and Evangelou E K 2011 *IEEE T. Electron Dev.* **58** 3549
[38] Xu J P, Lai P T, Li C X, Zou X and Chan C L 2006 *IEEE Electron Dev. Lett.* **27** 439
[39] Terman L M 1962 *Solid-State Electron.* **5** 285